



The influence of the support modification over Ni-based catalysts for dry reforming of methane reaction

Agnieszka Pietraszek*, Bachar Koubaissy, Anne-Cécile Roger, Alain Kiennemann

LMSPC, Laboratoire de Matériaux, Surfaces et Procédés pour la Catalyse, UMR 7515 du CNRS-ECPM-ULP, 25 Rue Becquerel, 67087 Strasbourg Cedex 2, France

ARTICLE INFO

Article history:

Received 1 September 2010

Received in revised form 7 December 2010

Accepted 8 December 2010

Available online 5 January 2011

Keywords:

CO₂ reforming of CH₄

Ni

Ru

Rh

Carbon formation

ABSTRACT

5 wt.%Ni/CeZr0.5 wt.%Me (Rh,Ru) catalysts were synthesized by mixed sol–gel and impregnation method. Their catalytic activity was examined in dry reforming of methane reaction (DR) and compared with CeZrMe (Rh,Ru) parent catalysts prepared by sol–gel method. The as prepared fresh catalysts were characterized by XRD while the aged catalysts by XRD, TPO, TEM and Raman. It was found that the Rh and Ru were well incorporated into CeZr fluorite structure. Nickel was present in NiO form.

Ni/CeZrRh catalyst demonstrated the highest activity reaching at 800 °C CH₄ conversion near thermodynamic one.

Ageing of the catalysts shows that the introduction of Rh into CeZr structure results in high activity and good stability even without Ni addition. However for CeZrRu catalyst deactivation is observed. The subsequent impregnation of Ni over CeZrRu catalyst leads to the considerable increase in its stability.

© 2010 Elsevier B.V. All rights reserved.

1. Introduction

The natural gas can be enriched through its transformation into synthesis gas (CO + H₂) by several routes. One of them is dry reforming of methane (DR), which allows the utilization of the excess of CO₂ present in some natural gas streams. The equilibrium composition of an endothermic DR reaction is influenced by the presence of the reverse water gas shift (RWGS) reaction and by coke formation. The occurrence of RWGS results in a decrease in H₂/CO ratio providing the ratios below thermodynamically admissible value of 1.

Coking is the principal way of deactivation of DR catalysts. It can be accomplished via Boudard reaction and/or CH₄ decomposition [1].

To minimize coke formation two approaches can be taken into account. The first one can be executed by working at high temperatures [2], low space velocities [3] or diluting reaction mixture [4]. The second approach can be allied with the modifications in catalysts composition. CeZr seems to be very attractive as a support due to its good thermal resistance and high mobility of oxygen what can facilitates the reaction with adsorbed carbon species [5]. It was demonstrated that the incorporation of small amount of metal into CeZr structure [6,7] results in shifting of reduction temperature of active metal and CeZr support to lower values what in the end can

influence the hindering of CH₄ decomposition reaction and thus coke formation.

It is generally known that nickel-based catalysts are very interesting in DR reaction due to their lower cost and higher availability [2,8–10]. Nevertheless, these catalysts are needed to be improved in terms of deactivation due to coke formation. Noble metals (i.e. Rh, Ru) reach high activity with a high coke resistance but they are less attractive in view of their costs [11]. The addition of noble metals assists Ni reducibility acting through a hydrogen spill-over [12], which brings H-atoms to the active metal [13,14].

The aim of this paper is to investigate the promoting effect of incorporation of small amount (0.5 wt.%) of noble metals (Ru and Rh) into CeZr structure and its impact over Ni-impregnated CeZrMe (Rh,Ru) catalysts. The influence of modification in Ni catalysts over its activity, coke formation and ageing process is evaluated.

2. Experimental

2.1. Catalyst preparation

Two different synthesis methods were involved into catalysts' preparation. The CeZr support as well as modified by 0.5 wt.% of noble metal CeZrRh and CeZrRu parent catalysts were developed by using pseudo sol–gel method based on thermal decomposition of metallic propionates [6,15,16].

The introduction of 5 wt.% of Ni was conducted by wet impregnation in the excess of the solvent. The precursor used was nickel (II) nitrate hexahydrate. The obtained dry residue was calcined in air at 750 °C during 4 h. The catalysts formulations are sum-

* Corresponding author.

E-mail addresses: pietraszek@unistra.fr, agnieszka.pietraszek12@gmail.com (A. Pietraszek).

marized as follows $\text{Ce}_2\text{Zr}_2\text{O}_8$ (CeZr), $\text{Ce}_2\text{Zr}_{1.97}\text{Rh}_{0.03}\text{O}_{8-\delta}$ (CeZrRh), $\text{Ce}_2\text{Zr}_{1.97}\text{Ru}_{0.03}\text{O}_{8-\delta}$ (CeZrRu), 5 wt.%Ni/CeZr $_{1.97}\text{Rh}_{0.03}\text{O}_{8-\delta}$ (Ni/CeZrRh) and 5 wt.%Ni/CeZr $_{1.97}\text{Ru}_{0.03}\text{O}_{8-\delta}$ (Ni/CeZrRu).

2.2. Catalysts' characterization

The catalyst phase composition was determined by Powder X-Ray Diffraction (XRD) on Brucker D8 Advanced diffractometer with Cu K α radiation.

Thermoprogrammed oxidation (TPO) was conducted over aged catalysts heated from room temperature to 900 °C with a slope 15 °C/min in the oxygen/helium mixture. CO $_2$ formation was analyzed by Mass Spectrometer Pfeiffer Vacuum. The catalyst surface was previously pre-heated in helium to decompose possible carbonates presented on the surface and to be sure that all CO $_2$ formed during TPO comes only from the carbon oxidation.

Transmission Electron Microscopy images were collected by TOPCON EM-002B apparatus with accelerating voltage 200 kV. The specimens for TEM were prepared by the dispersion of a small amount of the samples in ethanol and depositing them on membrane supported on copper grids.

Raman spectra were recorded using a Micro-Raman set-up (DILORXY), back-scattering geometry.

2.3. Catalytic activity

The catalytic activity measurements were performed in a fixed bed quartz reactor. Prior to CO $_2$ /CH $_4$ reaction, 0.1 g of catalyst was reduced in 5% H $_2$ –95% Ar at 750 °C for 4 h (0.0025 L/min). After the pre-treatment, a feed mixture consisted of CH $_4$ /CO $_2$ /Ar 10/10/80 was introduced into reactor. The total space velocity was equal to 30 L h $^{-1}$ g $^{-1}$. The reforming tests were studied with an increase of temperature from 550 °C to 800 °C with the stabilization of 2 h at each temperature. Some steady-state experiments at 750 °C were also performed to study the stability of the catalysts. The effluent gases were analyzed by micro Gas Chromatograph (Agilent) equipped with two columns: Poraplot U and Tamis 5A.

3. Results and discussion

3.1. Catalysts characterization

XRD diffractograms of the freshly prepared catalysts and support (Fig. 1) show the patterns matching well to face-centered cubic structure of solid solution of Ce $_{0.6}\text{Zr}_{0.4}\text{O}_2$ (JCPDS 38-1439). The patterns characteristic to ruthenium or rhodium oxides were not detected in the catalysts prepared by sol–gel method. The ionic radii of Rh (Rh $^{3+}$ 67 pm) is close to ionic radii of Zr (Zr $^{4+}$ 84 pm). Sol–gel preparation facilitates the incorporation of metal in low concentration into CeZr structure [6,7]. As the ionic radii of Ru $^{3+}$ is 68 pm the insertion of this metal into CeZr structure was also observed.

It should be noticed also that for the impregnated catalysts the patterns characteristic of nickel oxide (JCPDS 01-089-7131) are present (Fig. 1). For impregnated catalyst all Ni is outside the CeZr structure containing Rh and Ru what can be confirmed by the lack of change in lattice parameters compared to CeZr alone with the same Ce/Zr ratio (5.30 Å).

3.2. Catalytic activity measurements

It was demonstrated that the optimal Ce to Zr ratio was equal to 50:50 to obtain catalysts with high activity and good stability [6]. Fig. 2A shows the comparison of CH $_4$ conversion versus temperature for CeZr, CeZrMe (Rh,Ru) and 5 wt.%Ni/CeZrMe (Rh,Ru)

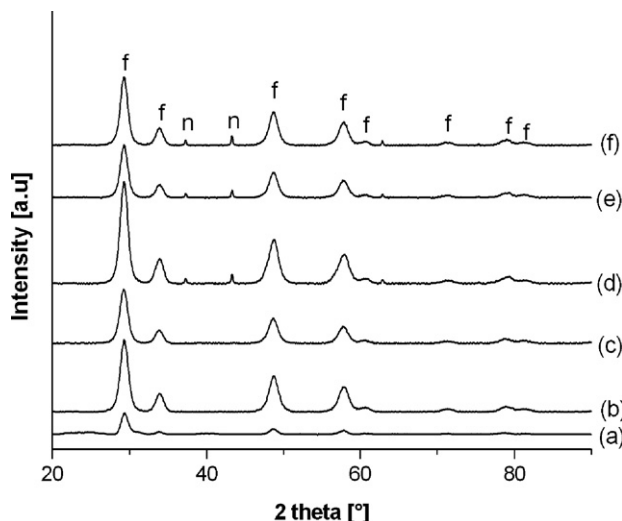


Fig. 1. XRD of freshly prepared catalysts (a) CeZr, (b) Ni/CeZr, (c) CeZrRh, (d) CeZrRu, (e) Ni/CeZrRh and (f) Ni/CeZrRu; f – face centered cubic fluorite structure, n – NiO species.

catalysts with the thermodynamic curve. The conversion values corresponding to thermodynamic equilibrium were obtained by the simulation (minimization of Gibbs energy) using program ProSim Plus. It can be seen that the conversions obtained experimentally are always below thermodynamic values. The introduction of Ru or Rh into CeZr fluorite structure results in augmentation in catalyst activity. The increase in CH $_4$ conversion at 750 °C from 2% in the case of CeZr support to 59% for CeZrRu and 82% for CeZrRh catalyst was observed. It can be seen that the insertion of Rh leads to the highest changing in catalytic properties, achieving the activity close to the thermodynamic equilibrium. The impact of Ni impregnation over CeZr and CeZrRu and CeZrRh parent catalysts shows a subsequent increase of activity up to 76% and 85% respectively while for Ni/CeZrRh slightly to 87%. The methane consumption is generally lower than one of CO $_2$ what can be assigned to the occurrence of reverse water gas shift reaction (RWGS) appearing simultaneously with dry reforming of methane. Donazzi et al. [17] suggests that dry reforming of methane is a combination of steam reforming and RWGS reactions. This can be confirmed by H $_2$ /CO ratio curves (Fig. 3). Their growth with the increase of temperature can be explained by the augmentation in selectivity towards hydrogen. In the case of CeZrRh, Ni/CeZr and Ni/CeZrRu catalysts the hydrogen to carbon monoxide ratio is higher than unity what can be associated with the presence of methane decomposition and/or steam reforming of methane. Some long term tests were also performed to study the stability and deactivation of CeZrRh, CeZrRu, Ni/CeZr, Ni/CeZrRu and Ni/CeZrRh catalysts (Fig. 2B). The experiments were performed at 750 °C during 90 h (for Ni/CeZr only 70 h due to its rapid deactivation). The catalysts exhibit a good stability in CH $_4$ conversion except CeZrRu and Ni/CeZr for which drop of more than 40% was observed. The introduction of Rh into CeZr structure results in good stability even without Ni addition. However for CeZrRu the impregnation of Ni leads to the considerable increase in its stability compared to CeZrRu parent catalyst.

3.3. Characterization after test

3.3.1. Physico-chemical characterization

After catalytic tests the fluorite structure is always present without changing in lattice parameters (ca. 5.30 Å). The diffraction patterns (Fig. 4) at 2 θ = 45° and 50° are indexed as Ni metal for Ni-

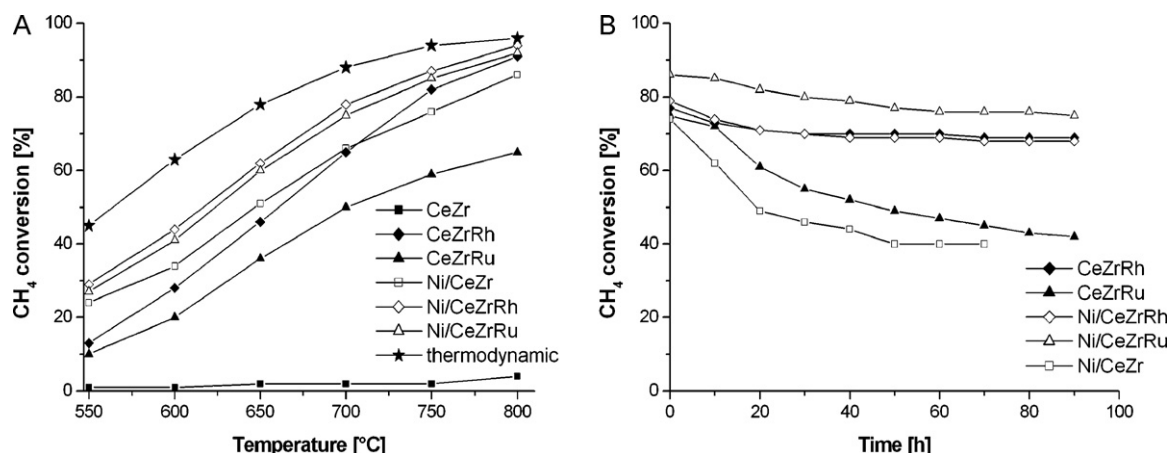


Fig. 2. (A) CH₄ conversion over different catalysts. Reaction conditions: CH₄/CO₂/Ar 10/10/80; total space velocity equal to 30 L/h/g; catalyst pretreatment before reaction: reduction in H₂/Ar 5/95 at 750 °C/4 h and (B) CH₄ conversion versus time during stability test at 750 °C over sol-gel and impregnated sol-gel catalysts. Reaction conditions: CH₄/CO₂/Ar 10/10/80; total space velocity equal to 30 L/h/g; catalyst pretreatment before reaction: reduction in H₂/Ar 5/95 at 750 °C/4 h.

containing catalysts however noble metals (Rh, Ru) are never seen due to their low concentration (0.5 wt.%).

3.3.2. Carbon evaluation

The main cause of the catalysts deactivation during dry reforming of methane is coke caused by a lack of equilibrium between carbon formation and removal reactions. There are several types of carbon species like adsorbed amorphous carbon, bulk metal carbide, crystalline graphite and filaments. Moreover carbon deposits can encapsulate active metal particles. TPO profiles of CeZrRh, CeZrRu and Ni/CeZr catalysts (Fig. 5) show CO₂ peak at ca. 600 °C. This peak was assigned to the presence of carbon in the form of nanotubes or fiber structure [18,19]. It was observed that the incorporation of Rh or Ru into CeZr structure results in increase in coke formation compared with Ni/CeZr catalyst (5×10^{-6} mol C/mol C transformed for CeZrRh, 9×10^{-6} mol C/mol C transformed for CeZrRu and 2×10^{-6} mol C/mol C transformed for Ni/CeZr). In Fig. 5 the curve corresponds to Ni/CeZr associates with the catalyst aged 70 h while the other two with the catalysts aged 9 h.

The TEM images show the presence of two kinds of carbon deposits (Fig. 6A–D). In the case of Ni-free catalysts surface carbon was observed while for Ni supported catalysts – carbon nanotubes.

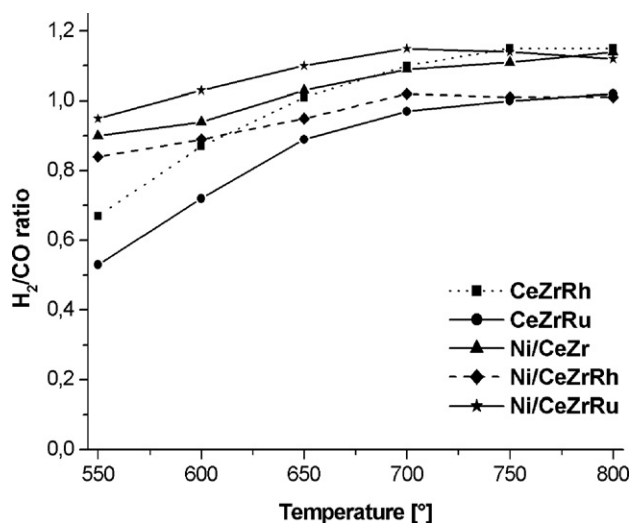


Fig. 3. H₂/CO ratio over different catalysts. Reaction conditions: CH₄/CO₂/Ar 10/10/80; total space velocity equal to 30 L/h/g; catalyst pretreatment before reaction: reduction in H₂/Ar 5/95 at 750 °C/4 h.

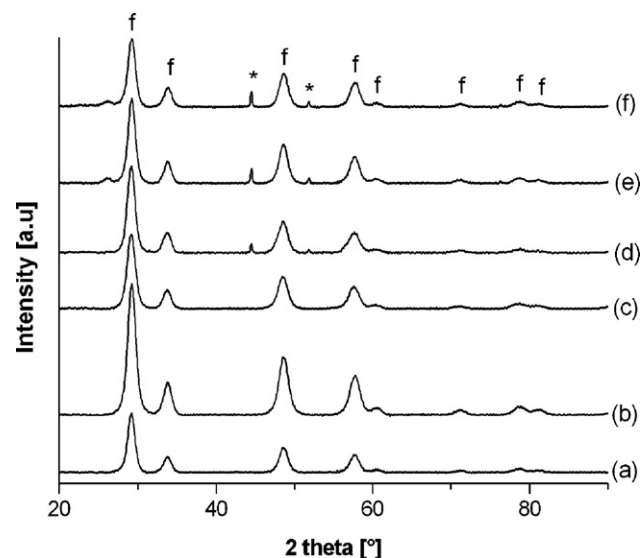


Fig. 4. XRD of aged catalysts used in reaction conditions: CH₄/CO₂/Ar 10/10/80; total space velocity equal to 30 L/h/g; catalyst pretreatment before reaction: reduction in H₂/Ar 5/95 at 750 °C/4 h; (a) CeZr, (b) CeZrRh, (c) CeZrRu, (d) Ni/CeZr, (e) Ni/CeZrRh and (f) Ni/CeZrRu; f – face centered cubic fluorite structure, * – Ni species.

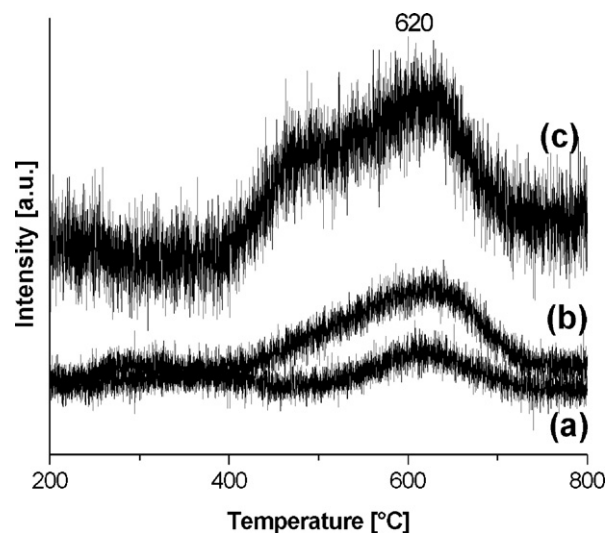


Fig. 5. TPO profiles of (a) CeZrRh, (b) CeZrRu, (c) Ni/CeZr catalysts after long term reaction at 750 °C.

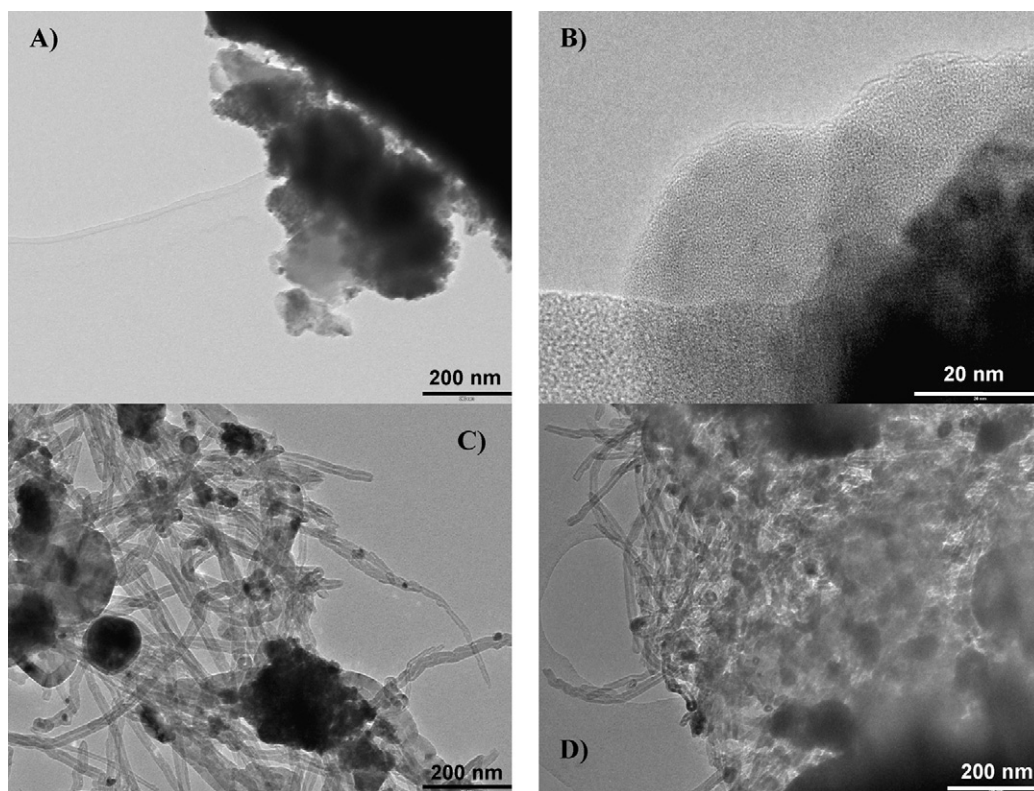


Fig. 6. TEM images of spent catalysts after long-term test at 750 °C during 90 h. (A) CeZrRh, (B) CeZrRu, (C) Ni/CeZrRh and (D) Ni/CeZrRu. Reaction conditions: CH₄/CO₂/Ar 10/10/80; total space velocity equal to 30 L/h/g; catalyst pretreatment before reaction: reduction in H₂/Ar 5/95 at 750 °C/4 h.

In the case of Ni/CeZrRu catalyst arising nanotubes are more compact than for the Ni/CeZrRh.

The Raman profiles (Fig. 7) were fitted to the G (1580 cm⁻¹) and D (1310 cm⁻¹) bands. Both bands are connected with the presence of structured carbon. The G band arises from the in-plane C–C stretching vibrations of the layers, while the D band is thought to originate from structural imperfections [20]. The peak observed at 470 cm⁻¹ can be attributed to CeO₂ [21]. In the case of Ni impregnated catalysts G and D bands are clearly visible and distinguish.

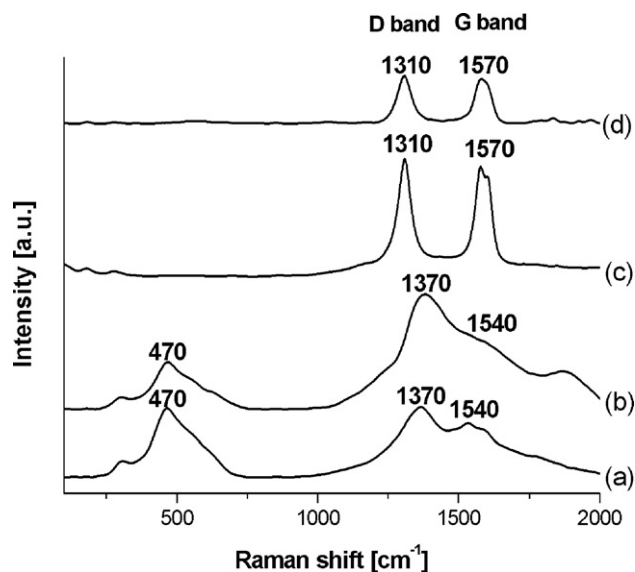


Fig. 7. Raman spectra of aged catalysts (a) CeZrRh, (b) CeZrRu, (c) Ni/CeZrRh and (d) Ni/CeZrRu after long-term test at 750 °C during 90 h.

Raman results are in accordance with TPO and TEM results where carbon nanotubes were observed. For CeZrRh and CeZrRu catalysts the G and D bands are seen but are not very well separated and are shifted to higher Raman shift in the case of D band and to lower Raman shift in the case of G band. The intensity ratio (I_D/I_G) of the D and G bands can be employed to measure the degree of graphite layers crystallinity. According to calculations it can be demonstrated that the lowest I_D/I_G ratio was observed for Ni/CeZrRu catalyst (1.05) and the highest for CeZrRh (1.17) with the middle value 1.12 for Ni/CeZrRh one. Low I_D/I_G ratio implicates the presence of less number of structural defects.

4. Conclusions

The catalysts were prepared by pseudo sol–gel and mixed sol–gel and impregnation methods. The XRD diffractograms of freshly prepared as well as aged catalysts match well to face-centered cubic fluorite structure without trace of Rh and Ru oxides. The NiO patterns were observed for the fresh Ni-containing catalysts while for spent catalysts metallic Ni has been seen. It was demonstrated that incorporation of Rh or Ru into CeZr structure increases the catalytic activity however the impregnation of Ni over such prepared materials results in subsequent improving, clearly observed for CeZrRu catalyst. The presence of noble metals (Rh, Ru) increases the stability of Ni/CeZr catalyst, whereas in the case of CeZrRh catalyst the addition of Ni did not change its resistance for deactivation.

Two types of carbon deposits were observed over examined catalysts, surface carbon in the case of CeZrMe (Ru,Rh) parent catalysts and carbon nanotubes in Ni/CeZrMe (Ru,Rh). The presence of structured carbon was also confirmed by Raman spectra by the occurrence of G (1580 cm⁻¹) and D (1310 cm⁻¹) bands.

Acknowledgements

The authors wish to acknowledge the support from Project *Era Chemistry*. The authors are also very grateful to Professor Phillipe Serp for Raman spectra.

References

- [1] L. Guzzi, G. Stefler, O. Geszti, I. Sajó, Z. Pászti, A. Tompos, Z. Schay, *Appl. Catal.* 375 (2010) 236.
- [2] X.S. Li, J.S. Chang, M.Y. Tian, S.E. Park, *Appl. Organometal. Chem.* 15 (2001) 109.
- [3] X. Li, L. Luo, K. Liu, *React. Kinet. Catal. Lett.* 77 (2001) 261.
- [4] H.S. Roh, H.S. Potdar, K.W. Jun, J.W. Kim, Y.S. Oh, *Appl. Catal. A* 276 (2004) 231.
- [5] A. Kambolis, H. Matralis, A. Trovarelli, Ch. Papadopolou, *Appl. Catal. A* 377 (2010) 16.
- [6] B. Koubaisy, A. Pietraszek, A.C. Roger, A. Kiennemann, *Catal. Today* 157 (2010) 436.
- [7] E. Ambroise, C. Courson, A.C. Roger, A. Kiennemann, G. Blanchard, S. Rousseau, X. Carrier, E. Marceau, C. La Fontaine, F. Villain, *Catal. Today* 154 (2010) 133.
- [8] D. Liu, R. Lau, A. Borgna, Y. Yang, *Appl. Catal. A* 358 (2009) 110.
- [9] Z. Hou, O. Yokota, T. Tanaka, T. Yashima, *Catal. Lett.* 87 (2003) 37.
- [10] H. Seok, S.H. Choi, E.D. Park, S.H. Han, J.S. Lee, *J. Catal.* 209 (2002) 6.
- [11] Y. Mukainakano, B. Li, S. Kado, T. Miyazawa, K. Okumura, T. Miyao, S. Naito, K. Kunimori, K. Tomishige, *Appl. Catal. A* 318 (2007) 252.
- [12] W.C. Conner, J.L. Falconer, *Chem. Rev.* 95 (1995) 759.
- [13] M.E. Rivas, J.L.G. Fierro, M.R. Goldwasser, E. Pietri, M.J. Perez-Zurita, A. Griboval-Constant, G. Leclercq, *Appl. Catal. A* 344 (2008) 10.
- [14] C. Crisafulli, S. Scire, S. Minico, L. Solarino, *Appl. Catal. A* 225 (2002) 1.
- [15] J.C. Vargas, E. Vanhaecke, A.C. Roger, A. Kiennemann, *Stud. Surf. Sci. Catal.* 147 (2004) 115.
- [16] F. Romero-Sarria, J.C. Vargas, A.C. Roger, A. Kiennemann, *Catal. Today* 133 (2008) 149.
- [17] A. Donazzi, A. Beretta, G. Groppi, P. Forzatti, *J. Catal.* 255 (2008) 259.
- [18] W. Pan, Ch. Song, *Catal. Today* 148 (2009) 232.
- [19] A. Horvath, G. Stefler, O. Geszti, A. Kiennemann, A. Pietraszek, L. Guzzi, *Catal. Today* (2010), doi:10.1016/j.cattod.2010.08.004.
- [20] C.A. Johnson, K.M. Thomas, *Fuel* 63 (1984) 1073.
- [21] S. Perres-Esclapez, I. Such-Basanez, M.J. Illan-Gomez, C. Salinas-Martinez de Lecea, A. Bueno-Lopez, *J. Catal.* 276 (2010) 390.